Design of a Phase-Locked-Loop-based Control Scheme for Lissajous-Trajectory Scanning of Fast Steering Mirrors

Ernst Csencsics and Georg Schitter

***Abstract*— This paper introduces an advanced phase-locked-loop (PLL) control structure for an electromagnetically actuated fast steering mirror (FSM). It enables a performance improvement when tracking Lissajous trajectories on a modified FSM. The dynamics of the FSM are inserted into the phase control loop of the PLL control structure, such that frequency and phase of the output and the reference signal are synchronized. Feedforward gains are used to enable matching of the output and reference scan amplitudes. It is shown that the PLL together with decoupling control blocks is also capable of compensating crosstalk between the FSM axes. The performance of the designed control system is compared to state of the art dual tone (DT) controllers for Lissajous trajectories. While both control structures show comparable current consumption, the resulting rms tracking error can be reduced by 60% when using the proposed PLL-based controls.**

I. INTRODUCTION

Fast steering mirrors (FSMs) are used in a variety of applications, which can be categorized into (i) pointing and (ii) scanning applications. Pointing applications include tasks such as acquisition of optical signals [1], tracking of objects [2] and beam stabilization in optical systems [3]. Typical examples for scanning applications are ranging from laser scanners [4], over scanning confocal microscopy [5] to scanning optical lithography [6], material processing [7] and optical free space communication [8]. FSMs are typically operated in closed-loop with high bandwidth feedback controllers [9], [10] and are actuated by piezoelectric [8], [11] and electromagnetic [3], [4] actuators, depending on the system requirements.

Focusing on 2-dimensional scanning applications raster trajectories are commonly employed patterns [7], [12], as also known from other scanning systems e.g. scanning probe microscopy [13]. They have multiple frequency components and require a high control bandwidth [17]. Lissajous-based scan trajectories are an alternative type of trajectory applicable to high precision scanning systems, such as atomic force micsocopes (AFMs) [14], optical microscopy [15] or medical imaging [16]. In contrast to a raster trajectory they result from driving each system axis with a sinusoidal signal of a single frequency. Recently it was shown that Lissajous trajectories can also be applied to FSM scanning systems [18]. In combination with dual tone (DT) controllers the Lissajous trajectory enables a reduction of the tracking error, as compared to a conventional raster trajectory tracked with a PID controller. Tuning the axis resonances to the trajectory frequencies further showed a reduction of energy consumption and enlargement of the scan area [19].

The authors are with the Christian Doppler Laboratory for Precision Engineering for Automated In-Line Metrology at the Automation and Control Institute Vienna University of Technology, 1040 Vienna, Austria. Corresponding author: csencsics@acin.tuwien.ac.at

When it comes to tracking of periodic signals phase locked loops (PLLs) are a wide spread and frequently used control scheme [20]. They keep an output signal synchronized with a reference input in frequency and thus minimize the resulting phase error [21]. Originally mainly used in the fields of communication systems [22], radio and television [20], PLLs have also been used in speed controllers for brushless DC (BLDC) motors [23]. Recently PLLs have been applied in a natural frequency tracking system for MEMS devices [24], [26], in AFMs to track spiral trajectories [25] and in resonant fiber scanners to track Lissajous trajectories [27].

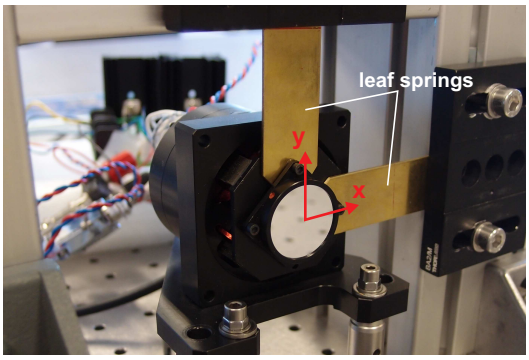

Fig. 1. Modified FSM system from Optics in Motion. Leaf springs are attached to the mover to tune the resonance frequencies of the axes to the targeted drive frequencies by changing the stiffness. They are mounted to mechanical ground.

Model-based controller designs require highly precise system models relying on system identification data, which is in general subjection to uncertainties in the gain and phase measurement. These uncertainties represent a potential limitation on the precision of the models and on the tracking performance for controllers tuned to distinct frequencies, such as the DT controller. This limitation can be avoided by employing a PLL which does not require a precise model of the system phase.

This paper proposes a PLL-based control structure for Lissajous-based scanning of electromagnetically actuated FSMs with the aim to further improve the tracking performance as compared to state of the art controllers [18]. In Section II the experimental setup is described, the derivation of the targeted Lissajous trajectory is explained and a system identification of the FSM is performed. Section III presents the design of the PLL-based control scheme and the deriva-

Post-print version of the article: Ernst Csencsics and Georg Schitter, "Design of a phase-locked-loop-based control scheme for Lissajous-trajectory scanning of fast steering mirrors," *2017 American Control Conference (ACC)*, pp. 1568-1573, 2017. DOI: 10.23919/ACC.2017.7963176

tion of the DT controllers. A comparison of the performance of the FSM with the PLL-based control and DT controllers is presented in Section IV by evaluating the tracking error and energy consumption when tracking the targeted Lissajous trajectory. Section V concludes the paper.

II. SYSTEM DESCRIPTION AND IDENTIFICATION

A. System Description

To investigate the PLL-based controls a commercial FSM (Type: OIM101, Optics in Motion LLC, Long Beach, USA) with an angular range of ±26.2 mrad (±1.5 deg) is used (see Fig. 1). Each FSM axis has a pair of voice coil actuators with static coils and moving magnets, working in a push-pull configuration. To measure the mirror rotation in two dimensions for closed-loop operation the FSM internal optical sensor system is used. The actuator coil pairs of each axis are driven by a custom made current amplifier (OPA544T, Texas Instruments Inc., Dallas, TX, USA) with a bandwidth of 10 kHz. The system is modified for energy efficient operation and resonant scanning by attaching leaf springs to each axis for individually tuning the resonance frequencies [19] (see Fig. 1). A dSpace system (DS1202, dSPACE GmbH, Germany) is used as control platform generating the amplifier inputs (x_{in} and y_{in}) and recording the sensor signals (x_{out} and y_{out}). Further it is used to implement a rotation matrix for transforming the drive signals, as the actuation and sensing axes of the FSM are 45° rotated with respect to each other.

B. Lissajous Trajectory Design

Considering an exemplary scientific scanning application with a typical image size of 300 x 300 pixel and a typical frame rate of 1 frame/s, a suitable Lissajous trajectory needs to be designed. Measurements with a capacitive sensor (Type: 6504, MicroSense LLC, Lowell, MA, USA; data not shown) revealed structural modes of the mirror carrier around 800 Hz that are not observable with the internal senor (see [19] for details). In the face of a precise scanning motion this represents an upper boundary condition for the drive frequency choice, as a deforming mirror mover would lead to deviations of the reflected beam that cannot be compensated. Two competing aims need to be considered for the choice of the two drive frequencies: (i) the difference between the frequencies needs to be small, in order to ensure good spatial resolution along the two principal axes, and (ii) the frequencies need to be well separated to reduce the crosstalk between both scanning axes [19]. As a trade-off for these requirements the drive frequencies should range between 700 Hz (about 10% lower than the first structural mode) and 400 Hz. The frequencies f_x=488 Hz and f_y=619 Hz are chosen from this range. They result in a spatial resolution of 0.0025 and 0.0032 (with respect to unity image size) for the two scanning axes, clearly enabling a 300 x 300 pixel image, and a trajectory duration of T=1 s (1 frame/s) [14].

C. System Identification

To identify the system dynamics a system analyzer (3562A, Hewlett-Packard, Palo Alto, CA, USA) is used. The input of the power amplifier (x_{in} and y_{in}) is considered as the system input and the signal of the internal sensor (x_{out} and y_{out}) is considered as the system output (see Fig. 4). The mirror, the amplifier and the internal sensor are thus together considered as the plant. Fig. 2 shows the measured transfer functions (TFs) of the x- and y-axis. The resonance

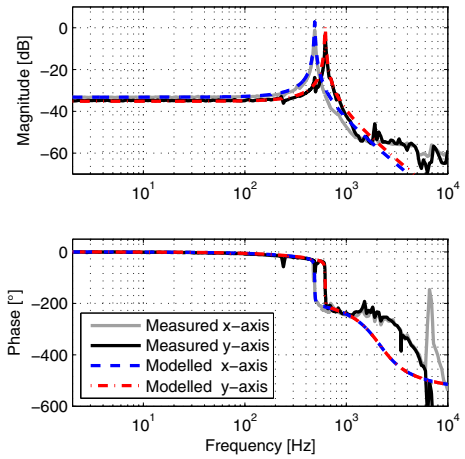

Fig. 2. Frequency response of the x- (solid grey) and y-axis (solid black) with the related system models (x - dashed blue, y - dash-dotted red). The resonance frequencies $f_{0x} = 488$ Hz and $f_{0y} = 619$ Hz of both axes are placed exactly at the targeted drive frequencies. The phase delay at higher frequencies results from the sampling delay of the digital system.

frequencies $f_{0x} = 488$ Hz and $f_{0y} = 619$ Hz are exactly adjusted to the drive frequency of each axis by tuning the flexures, resulting in plant gains of -1.2 dB and -4.2 dB, respectively. The noise floor of the system is at around -60 dB.

To model the measured frequency responses, second order models

$$G_{xx,yy}(s) = K \cdot \frac{\omega_0^2}{s^2 + 2\omega_0\zeta s + \omega_0^2} \cdot P_A(s), \qquad (1)$$

with identified parameters according to Table I are fitted to the data sets. The delay due to the sampling of the digital system at T_s=50 μs, is modeled by a second order Pade-approximation $P_A(s)$ [28] for the controller design. Minor structural modes due to the attached leaf springs at 230 and 500 Hz are omitted. The derived models are also depicted in Fig. 2. The slightly varying mass lines of the two axes result from the mounted leaf springs that add inertia to the mover.

Fig. 3 shows the measured crosstalk TFs of the FSM system with 4th order models G_{xy} and G_{yx} fitted around the two drive frequencies. As expected the largest crosstalk magnitudes are located around the resonance frequencies f_{0x} and f_{0y}. The crosstalk magnitudes are -17 dB at f_{0x}, and -33.5 dB (x-to-y) and -43 dB (y-to-x) at f_{0y}. At DC the crosstalk magnitude is about 17 dB smaller than the magnitude of the system axes, which in summary justifies

Post-print version of the article: Ernst Csencsics and Georg Schitter, "Design of a phase-locked-loop-based control scheme for Lissajous-trajectory scanning of fast steering mirrors," *2017 American Control Conference (ACC)*, pp. 1568-1573, 2017.
DOI: 10.23919/ACC.2017.7963176

TABLE I
PARAMETERS OF THE IDENTIFIED FSM SYSTEM MODELS.

Axis	Parameter	Value
x	K	0.0219
	ω_0	3.066e3 rad/s
	ζ	0.01
y	K	0.0174
	ω_0	3.889e3 rad/s
	ζ	0.01

the use of single input single output (SISO) controls for each axis.

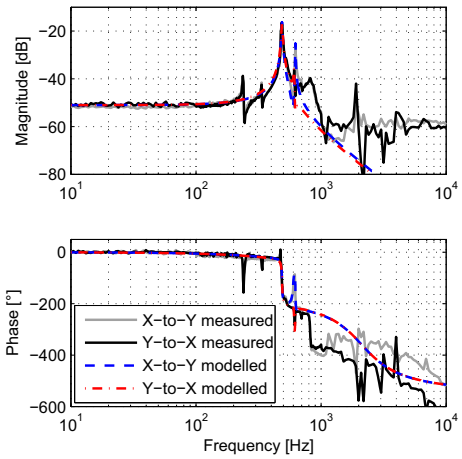

Fig. 3. Frequency response of the crosstalk from x-to-y- (solid grey) and from y-to-x-axis (solid black). The related 4th order models around the drive frequencies G_{xy} and G_{yx} are also depicted (x-to-y - dashed blue, y-to-x - dash-dotted red).

III. CONTROL DESIGN

Contrary to raster trajectories, comprising multiple frequency components, Lissajous-based trajectories result from driving each system axis with a single sinusoidal signal with a fixed frequency. This enables the use of tailored controller designs, such as DT controllers [18] or the proposed PLL-based control design.

A. PLL-based Control

A PLL is a control system that synchronizes the output signal of an oscillating system with a reference signal in terms of frequency and phase. It controls the phase of its output signal such that the phase error between output and reference reduces to a minimum [29]. A PLL typically consists of a phase detector (PD) a low pass filter (LP) and a voltage controlled oscillator (VCO). Let

$$u_r(t) = U_r \cdot sin\left(\omega_r t + \phi_r(t)\right), \quad (2)$$
$$u_o(t) = U_o \cdot cos\left(\omega_o t + \phi_o(t)\right) \quad (3)$$

be the reference and output signal that are applied to the PD, respectively. After all transients have vanished, assuming synchronized frequencies with ω_r=ω_o=ω and the phase error to be $\phi_e = \phi_r - \phi_o$, the output of the PD, which is essentially a multiplier, results to

$$u_{PD}(t) = U_r U_o \cdot \frac{1}{2}\left[sin\left(\phi_e\right) + sin\left(2\omega t + \phi_r + \phi_o\right)\right]. \quad (4)$$

The LP eliminates the high frequency component at 2ω, leaving a DC signal that is proportional to ϕ_e (assuming small angles) and that is applied to the VCO. The VCO is a frequency modulated oscillator with an output frequency ω_o that is a linear function of $u_{LP} = 1/2 \cdot U_r U_o \phi_e$ around its central frequency ω_c. The VCO adjusts the output frequency to minimize the phase error, and as $\omega = \frac{d}{dt}\phi$ the VCO represents an integrator for phase error signals. Further information on the details of PLLs and their treatment as linear systems in the case of steady state and small phase errors can be found in literature [20], [21], [29].

Each axis is equipped with a single PLL, as shown in Fig. 4), with the respective mechanical FSM axis (G_{xx} and G_{yy}) inserted into the loop after the VCO. Fig. 4 further depicts the built in optical position sensor *PS* of the FSM, the two current amplifiers, and the crosstalk TFs G_{xy} and G_{yx} of the mechanical system. The measured mirror position is fed back to the PD which modifies the VCO output, such that the phase of the output signal $\Theta_{x,y}$ (mirror position) matches the phase of the reference signal $\Theta_{x,y,ref}$. The center frequency ω_c of the VCO is set to the drive frequency of the related axis and the amplitude is set to the targeted reference amplitude. As the PLL is only controlling the phase, the gains g_x and g_y (see Fig. 4) succeeding the VCOs are added. These gains are determined by the inverse plant gain of the respective axis at the related drive frequency (cf. Fig. 2) to ensure good agreement of the output and reference amplitude. The used PLL structure is thus a pure phase feedback with gain feedforward.

B. Decoupling Control

The PLLs are, however, not capable of rejecting disturbances that result from crosstalk between the axes (G_{xy} and G_{yx}) and have frequency components at the drive frequency of the respectively other axis. Fig. 5a shows the simulated power spectral density (PSD) of the resulting tracking error, normalized to the largest PSD value, of the y-axis with only PLLs tracking the targeted Lissajous trajectory with f_x and f_y. It reveals major periodic error components at the drive frequency of the x-axis at 488 Hz and several small beat components. As the crosstalk behavior is, however, repeatable it can be seen as a measurable external disturbance, such that decoupling control (DCC), a variation of feedforward control, can be introduced to compensate these disturbances [30]. Decouplers to compensate the crosstalk are designed by using the results of the system identification from Section II-C

$$D_{xy}(s) = \left.\frac{G_{xy}(s)}{G_{yy}(s)}\right|_{s=j\omega_x}, D_{yx}(s) = \left.\frac{G_{yx}(s)}{G_{xx}(s)}\right|_{s=j\omega_y} \quad (5)$$

with G_{xy} and G_{yx} being the models of the crosstalk frequency responses. The entire PLL-based control structure with DCC

Post-print version of the article: Ernst Csencsics and Georg Schitter, "Design of a phase-locked-loop-based control scheme for Lissajous-trajectory scanning of fast steering mirrors," *2017 American Control Conference (ACC)*, pp. 1568-1573, 2017.
DOI: 10.23919/ACC.2017.7963176

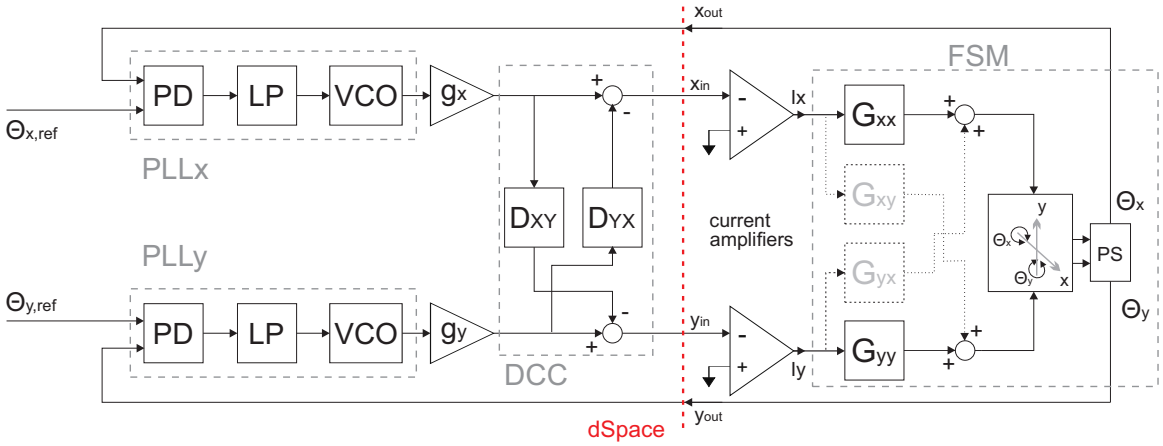

Fig. 4. Phase locked loop based control structure for the tracking of Lissajous trajectories. The phase of the output signal is synchronized with the input signal by one PLL per axis (PLL_x and PLL_y). The gains g_x and g_y are the inverted plant gains at the respective drive frequency to scale the amplitude of the output signal to the amplitude of the reference. The DCC blocks D_{xy} and D_{yx} are used to remove the crosstalk at the drive frequencies.

blocks is shown in Fig. 4. In contrast to positioning applications that evaluate DCC Blocks for DC (s=0) [30] the DCC Blocks for the Lissajous trajectory are evaluated at the respective drive frequency, resulting in single gain and phase values used to compensate crosstalk only at this frequency. Fig. 5b depicts the normalized (to the largest PSD value with PLLs only) PSD of the tracking error of the y-axis with PLLs and DCC blocks, showing that the crosstalk components can be entirely compensated.

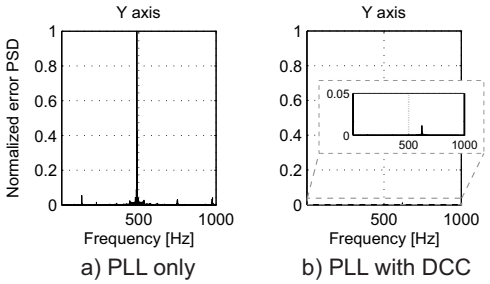

Fig. 5. Comparison of simulated normalized (to the largest value with PLL only) PSDs of the resulting tracking error of the y-axis using (a) only PLL control and (b) PLL control with DCC blocks. The system tracks a Lissajous trajectory with frequencies of 488/619 Hz. It can be seen that with the DCC blocks the crosstalk components can be compensated. The remaining error component at the drive frequency of the y-axis results from deviations at the maximum value of the driving sine signal.

C. Dual Tone Control

The design of the DT controllers for the two system axes follows exactly the design procedure described in [19], [18], and is based on an H_∞-approach [28]. This controller type is characterized by high gains peaks tuned to the two driving frequencies of the system, while showing low gain at all other frequencies. It is thus able to track a sinusoidal reference at one desired frequency with each axis and to cancel crosstalk at the drive frequency of the respectively other axis. It was shown that DT controllers can be used to reduced the tracking error compared to a classical PID controller by a factor of 50 when tracking a Lissajous trajectory [18]. Using the system models from Section II-C in the design procedure and applying the weighting functions with two inverse notches (at the drive frequencies) for the sensitivity and an inverse low pass for the input sensitivity function the controllers are derived. Both controllers show highly localized control efforts around the drive frequencies with the largest effort at the drive frequency of the respectively other axis, due to the increased plant gain at the resonances.

D. Implementation

The PLL structure is implemented in the dSpace system for a sampling frequency of f_s=20 kH. The PD is realized as simple multiplier and the LP is a first order low pass filter with a bandwidth of 10 Hz [29]. The inverse plant gains g_x and g_y are implemented with an adaptive tuning algorithm, so that no identification data is required. After decay of the PLL's transients the algorithm is activated and minimizes the rms error between a 90°-phase-shifted reference and the output signal, being proportional to the gain mismatch.

As pointed out in Section III-B the TFs of the DCC blocks are evaluated at the drive frequency of each axis only. Fig. 6 shows a comparison of the measured crosstalk from y- to x-axis in the time domain with only the y-axis actuated and the DCC blocks switched on and off, respectively. It can be seen that the crosstalk from y- to x-axis with active DCC blocks can be significantly reduced from -13 dB to -43 dB. The crosstalk from x- to y-axis is reduced to below -50 dB.

For implementation on the dSpace system the DT controllers for both system axes are discretized using Pole-Zero-Matching [31] for a sampling frequency of f_s=20 kHz. The complementary sensitivity functions show high tracking performance at the two drive frequencies only, where they reach the 0 dB line and roll-on and-off steeply before and

Post-print version of the article: Ernst Csencsics and Georg Schitter, "Design of a phase-locked-loop-based control scheme for Lissajous-trajectory scanning of fast steering mirrors," *2017 American Control Conference (ACC)*, pp. 1568-1573, 2017.
DOI: 10.23919/ACC.2017.7963176

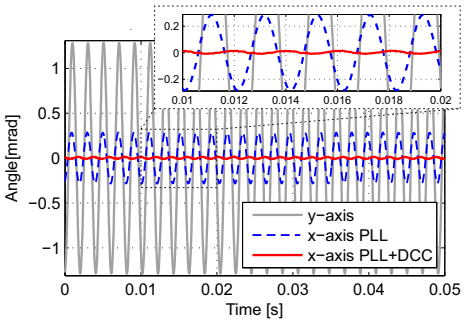

Fig. 6. Measured crosstalk from y- to x-axis with y-axis driven with a scan amplitude of 1.31 mrad and the DCC blocks disabled (blue) and enabled (red), respectively. With the DCC blocks active the crosstalk can be reduced from -13 dB to -43 dB.

after. By introduction of non-minimum phase zeros in the controller, good phase matching is achieved at the drive two frequencies f_x and f_y [19].

IV. EXPERIMENTAL RESULTS

For investigation of the closed-loop performance of the two control structures, both systems are tracking the targeted Lissajous trajectory (see Section II-B) for different scan amplitudes. To evaluate the current consumption the sum rms current through both coils is measured. The scan amplitudes are increased until the current limit of the coils is reached. The internal sensor is used for position measurement and the spatial tracking error is calculated by taking the euclidean distance from reference to measured trajectory in every sampling point.

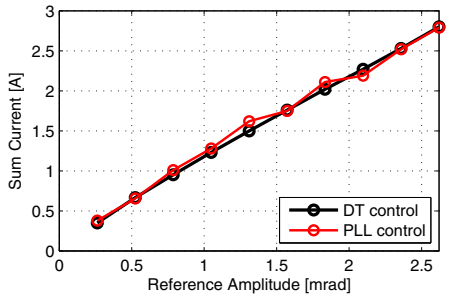

Fig. 7. Comparison of the rms drive current for both axes using the DT (black) and PLL controls (red) at different reference amplitudes. Both control structures require the same amount of drive current over the entire scan amplitude range, reaching the current limit at a scan amplitude of 2.62 mrad.

Fig. 7 shows a comparison of the current consumption of the DT controlled (black slope) and the PLL controlled (red slope) FSM. It can be seen that the required current to track the Lissajous trajectory with the targeted scan amplitude is very similar over the entire range of feasible scan amplitudes. The current consumption increases linearly with the amplitude at about 1.2 A/mrad. The maximum scan amplitude is in both cases 2.62 mrad. Both control structures thus clearly achieve the same performance in terms of energy consumption and scan range.

Fig. 8 depicts the resulting spatial rms tracking errors of control structures at different scan amplitudes. The DT controlled FSM (black slope) shows an error around 2.5% of the scan amplitude over most of the feasible scan amplitude range. The PLL controlled FSM (red slope) shows an rms error of about 1% above 0.5 mrad. This implies that the resulting tracking error with PLL controls is 60% smaller than in the DT controlled case.

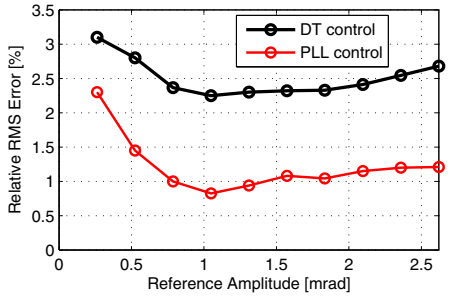

Fig. 8. Comparison of the resulting rms tracking error using the DT (black) and PLL controls (red) at different drive amplitudes. The error is related to the scan amplitude and ranges around 2.5% for larger scan amplitudes when DT controls are used. The rms error when using PLL controls ranges around 1% for larger scan amplitudes and is thus 60% smaller than the error when DT controls are used.

In Fig. 9 measured Lissajous scans are shown, demonstrating the improved tracking performance using PLL controls, as compared to DT controls. It can be seen that the agreement of reference and measured output trajectory is clearly enhanced over the entire scan area when using PLL controls.

In summary, the proposed PLL-based control structure with decoupling control blocks can be applied for high resolution Lissajous scanning of FSMs, improves the tracking performance by 60% and offers the same scan range as compared to state of the art DT controllers.

V. CONCLUSION

In this paper an advanced PLL-based control structure is introduced to improve the performance of electromagnetically actuated FSM scanning systems for tracking Lissajous trajectories. Exploiting the property of single frequency sinusoidal reference signals one PLL per axis is used to synchronize the output of the mechanical plant and the reference signal in terms of frequency and phase. Feedforward gains derived by an adaptive algorithm are tuned to the inverse plant magnitudes at the drive frequencies to ensure matching of reference and output amplitudes. To compensate the crosstalk between the system axes feedforward decoupling blocks are introduced. A comparison of the performance between the PLL controls and state of the art DT controllers [18] when tracking the targeted Lissajous trajectory reveals that the resulting rms tracking error can be reduced by 60% when using the proposed PLL controls while both control structures show the same current consumption.

Post-print version of the article: Ernst Csencsics and Georg Schitter, "Design of a phase-locked-loop-based control scheme for Lissajous-trajectory scanning of fast steering mirrors," *2017 American Control Conference (ACC)*, pp. 1568-1573, 2017.
DOI: 10.23919/ACC.2017.7963176

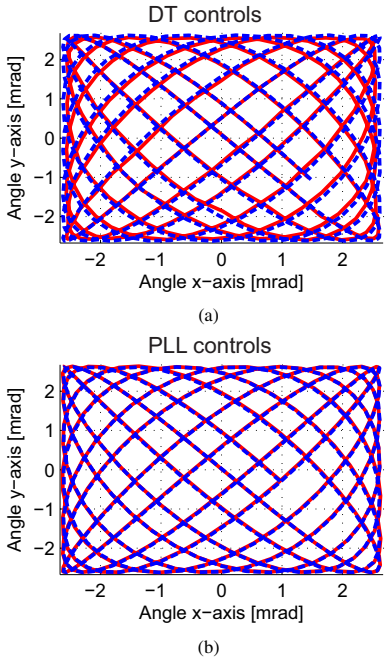

Fig. 9. Measured Lissajous scan with the target trajectory (1 frame/s) using (a) DT controls and (b) PLL controls. The figures depict the measured trajectory (solid red) and the reference trajectory (dashed blue) for a scan amplitude of 2.62 mrad and a time span of 15 ms. The improved tracking of the reference with PLL controls is clearly observable.

ACKNOWLEDGMENT

The financial support by the Austrian Federal Ministry of Science, Research and Economy and the National Foundation for Research, Technology and Development, as well as MICRO-EPSILON MESSTECHNIK GmbH & Co. KG and ATENSOR Engineering and Technology Systems GmbH is gratefully acknowledged.

REFERENCES

[1] M. Guelman, A. Kogan, A. Livne, M. Orenstein, and H. Michalik, Acquisition and pointing control for inter-satellite laser communications. IEEE Transactions on Aerospace and Electronic Systems, vol. 40, nr. 4, pp. 1239, 2004.
[2] S. H. Xiang, P. Wang, S. H. Chen, X. Wu, D. Xiao, and X. W. Zheng, The Research of a novel single mirror 2D laser scanner. International Symposium on Photoelectronic Detection and Imaging, pp. 73821A, 2009. International Society for Optics and Photonics.
[3] D. J. Kluk, M. T. Boulet, and D. L. Trumper, A high-precision, two-axis steering mirror with moving iron actuator. Mechatronics, vol. 22, no. 3, pp. 257, 2012.
[4] M. Hafez, T.C. Sidler, R.P. Salathe, G.L.M. Jansen, and J.C. Compter, Design, simulations and experimental investigations of a compact single mirror tip/tilt laser scanner. Mechatronics, vol. 10, no. 7, pp. 741, 2000.
[5] H.W. Yoo, M. E. van Royen, W. A. van Cappellen, A. B. Houtsmuller, M. Verhaegen, and G. Schitter, Automated spherical aberration correction in scanning confocal microscopy. Review of Scientific Instruments, vol. 85, pp. 123706, 2014.
[6] Q. Zhou, P. Ben-Tzvi, D. Fan, and A. Goldenberg, Design of Fast Steering Mirror systems for precision laser beams steering. International Workshop on Robotic and Sensors Environments, pp. 144, 2008. IEEE.
[7] L. R. Hedding and R. A. Lewis, Fast steering mirror design and performance for stabilization and single axis scanning. presented at International Society for Optics and Photonics Orlando '90, Orlando, FL, pp.14, 1990.
[8] H. Mokbel, W. Yuan, L. Qiong Ying, C. Guo Hua, and A. A. Roshdy, Research on the Mechanical Design of Two-Axis Fast Steering Mirror for Optical Beam Guidance. 1st International Conference on Mechanical Engineering and Material Science, Atlantis Press, 2012.
[9] Y.-X. Xia, Q.-L. Bao, and Q.-Y. Wu, Internal model control of a fast steering mirror for electro-optical fine tracking, Proc. of SPIE, vol. 7843, 2010.
[10] A. Berta, L. Hedding, C. Hoffman, and M. Messaros, Development of a commercial line of high-performance, fast-steering mirrors, Proc. of SPIE vol. 3787, pp. 181192, 1999.
[11] F. M. Tapos, D. J. Edinger, T. R. Hilby, M. S. Ni, B. C. Holmes, and D. M. Stubbs, High bandwidth fast steering mirror. Optics and Photonics, pp. 587707, 2005. International Society for Optics and Photonics.
[12] S. Xiang, S. Chen, X. Wu, D. Xiao, and X. Zheng, Study on fast linear scanning for a new laser scanner. Optics and LASER technology, vol. 41, no. 1, pp.42, 2010.
[13] G.Schitter, P.J. Thurner, and P. Hansma, Design and input-shaping control of a novel scanner for high-speed atomic force microscopy. Mechatronics, vol. 18, no. 5, pp. 282, 2008.
[14] T. Tuma, J. Lygeros, V. Kartik, A. Sebastian and A. Pantazi, High-speed multiresolution scanning probe microscopy based on Lissajous scan trajectories. Nanotechnology, vol. 23, no. 18, pp. 185501, 2012.
[15] S. Z. Sullivan, R. D. Muir, J. A. Newman, M. S. Carlsen, S. Sreehari, C. Doerge, N. J. Begue, R. M. Everly, C. A. Bouman, and G. J. Simpson, High frame-rate multichannel beam-scanning microscopy based on lissajous trajectories. Optics Express, vol. 22, no. 20, p. 24224, 2014.
[16] H. Feng, H. Gu, D. Silberzweig, E. Stern, and Y. Yang, Single-shot MR imaging using trapezoidal-gradient-based lissajous trajectories. IEEE Transactions on Medical Imaging, vol. 22, no. 8, p. 925, 2003.
[17] A. J. Flemming and A. G. Wills, Optimal periodic trajectories for band-limited systems. IEEE Transactions on Control Systems Technology, vol. 17, no. 3, pp. 552, 2009.
[18] E. Csencsics, R. Saathof and G. Schitter, Design of a dual-tone controller for Lissajous-based scanning of fast steering mirrors. Proceedings of the 2016 American Control Conference. IEEE, 2016.
[19] E. Csencsics and G. Schitter, System design and control of a resonant fast steering mirror for Lissajou-based scanning. IEEE Transactions on Mechatronics, submitted, 2016.
[20] D. Abramovitch. Phase-locked loops: A control centric tutorial. Proceedings of the 2002 American Control Conference IEEE, 2002.
[21] G.-C. Hsieh and J. C. Hung. Phase-locked loop techniques. A survey. IEEE Transactions on Industrial Electronics vol. 43, no. 6, pp. 609, 1996.
[22] D. R. Stephens. Phase-locked loops for wireless communications: digital, analog and optical implementations. Springer Science & Business Media, 2007.
[23] C. T. Pan and E. Fang. A phase-locked-loop-assisted internal model adjustable-speed controller for BLDC motors. IEEE Transactions on industrial electronics, vol. 55, no. 9, pp. 3415, 2008.
[24] X. Sun, R. Horowitz, and K. Komvopoulos. Stability and resolution analysis of a phase-locked loop natural frequency tracking system for MEMS fatigue testing. Journal of dynamic systems, measurement, and control, vol. 124, no.4, pp. 599, 2002.
[25] H. Habibullah, H. R. Pota, and I.R. Petersen. Phase-locked loop-based proportional integral control for spiral scanning in an atomic force microscope. IFAC Proceedings, vol. 47, no. 3, pp. 6563, 2014.
[26] A. Hung, H. Lai, T. Lin, S. Fu, and M. Lu. An electrostatically driven 2D micro-scanning mirror with capacitive sensing for projection display. Sensors and Actuators A: Physical, vol. 222, pp. 122, 2015.
[27] M. H. H. Mokhtar and R. R. A. Syms. Resonant fiber scanner with optical feedback. Optics express, vol. 22, no. 21, pp. 25629, 2014.
[28] S. Skogestad and I. Postlethwaite, Multivariable Feedback Control. John Wiley, New York, 2005.
[29] R. E. Best. Theorie und Anwendungen des Phase-locked Loops. AT & T. Bell, 1993.
[30] X. Zhou, D. Wang, J. Wang, S.-C. Chen. Precision design and control of a flexure-based roll-to-roll printing system. Precision Engineering, vol. 45, pp. 332, 2016.
[31] G. F. Franklin, D. J. Powell and M. L. Workman, Digital Control of Dynamic Systems. Prentice Hall, 1997.

Post-print version of the article: Ernst Csencsics and Georg Schitter, "Design of a phase-locked-loop-based control scheme for Lissajous-trajectory scanning of fast steering mirrors," *2017 American Control Conference (ACC)*, pp. 1568-1573, 2017. DOI: 10.23919/ACC.2017.7963176